

Acknowledgment. We gratefully acknowledge financial support from the Comisión Interministerial de Ciencia y Tecnología (CICYT) (Grant No. PPB86-0101) of Spain. We thank M. T. Compain for her technical assistance.

Registry No. 1, 129571-38-6; 2, 129571-39-7; 3, 129571-40-0; 4, 129571-41-1; *exo*-(*E*)-5, 129571-42-2; *exo*-(*Z*)-5, 129646-63-5; *exo*-(*E*)-6, 129571-43-3; *exo*-(*Z*)-6, 129646-64-6; 9, 129571-44-4; 10, 129571-45-5; Nb(η^5 -C₅H₅SiMe₃)₂Cl, 116852-35-8; Nb(η^5 -C₅H₄SiMe₃)₂Br, 125821-09-2; C₆H₅N=C=C(C₆H₅)₂, 14181-84-1;

p-CH₃C₆H₄B=C=C(C₆H₅)₂, 5110-45-2; C₆H₅B=C=C(CH₃)C₆H₅, 32907-79-2.

Supplementary Material Available: Listings of fractional coordinates, anisotropic thermal parameters, all bond distances and bond angles, torsion angles, least-squares planes, and interatomic and intermolecular contacts for 1 and the EPR spectrum of 9 (23 pages); a listing of the observed and calculated structure factors for 1 (20 pages). Ordering information is given on any current masthead page.

Low-Temperature Photochemistry of Oxy-Substituted Trisilanes

Gregory R. Gillette, George Noren, and Robert West*

Department of Chemistry, University of Wisconsin—Madison, Madison, Wisconsin 53706

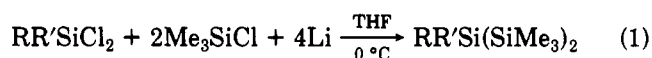
Received June 7, 1990

Several new oxy-substituted trisilanes RO(Mes)Si(SiMe₃)₂ were synthesized and photolyzed in hydrocarbon matrices at 77 K to give silylenes, RO(Mes)Si. The silylenes with R = mesityl and 2,6-diisopropylphenyl showed UV spectra that varied with matrix viscosity, attributed to conformational changes as the silylene relaxed to its equilibrium geometry. The structures of the two hindered (aryloxy)trisilanes **2a** and **2c** were determined by X-ray crystallography. Crystal data: **2c**, R = phenyl, *a* = 16.609 (3) Å, *b* = 18.081 (3) Å, *c* = 20.029 (3) Å, orthorhombic, *Pbca*, *Z* = 8; **2a**, R = 2,6-diisopropylphenyl, *a* = 13.078 (2) Å, *b* = 12.054 (3) Å, *c* = 15.111 (3) Å, β = 102.05 (1)°, monoclinic, *P2₁/c*, *Z* = 4. Their geometries about the central silicon atom were related to the UV properties of their respective silylenes. The solution-phase irradiation of the trisilane with R = 2,6-diisopropylphenyl at -60 °C led to the isolation of the first heteroatom-substituted cyclotrisilane, [RO(Mes)Si]₃, whose structure was determined by X-ray crystallography: space group *P* $\bar{1}$, *a* = 15.541 (2) Å, *b* = 17.707 (3) Å, *c* = 11.989 (2) Å, α = 109.70 (1)°, β = 109.60 (1)°, γ = 78.86 (1)°, *Z* = 2.

The understanding of silylene chemistry has increased significantly in the last decade with the application of matrix isolation techniques to the study of these very reactive species.¹ In this paper we report studies of several oxy-substituted silylenes, **3a-f**, obtained by the photolysis of the corresponding trisilanes **2a-f** at 77 K in hydrocarbon matrices and in solution at low temperatures.²

Results and Discussion

Synthesis of Oxy-Substituted Trisilanes. Linear trisilanes RR'Si(SiMe₃)₂, which are good photochemical precursors to silylenes,^{1,2} can often be made by coupling dichlorosilanes RR'SiCl₂ with trimethylchlorosilane in THF as shown in eq 1.³ However, attempts to make

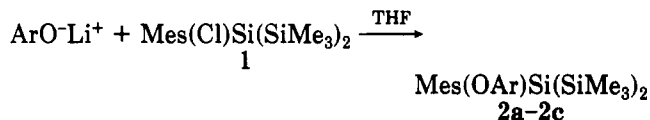


oxy-substituted trisilanes by this route all failed. The oxy group was displaced in preference to Cl in some reactions, and in every case, the major trisilane product had no oxy group remaining. Synthesis of the appropriate trisilanes was achieved by starting from 2-mesityl-2-chloro-

Table I. Absorption Maxima of Silylenes **3a-f** in Various Matrices

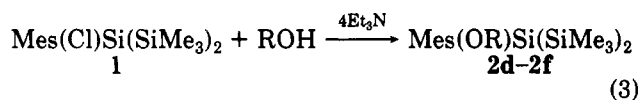
silylene	λ_{max} , nm	
	3-MP	1:1 3-MP/isopentane
3a	430	398
3b	425	400
3c	400	400
3d	390	390
3e	395	395
3f	396	396

1,1,1,3,3,3-hexamethyltrisilane (1). For aryloxy-substituted trisilanes, the best results were obtained by reacting the (aryloxy)lithium reagent with 1 in THF as shown in eq 2.



2a, Ar = 2,6-diisopropyl; **2b**, Ar = mesityl;
2c, Ar = phenyl (2)

Use of alkoxide ions in place of aryloxy in the reaction shown by eq 3 led to cleavage of Si-Si bonds. Alkoxy-trisilanes **2d-2f** were therefore synthesized by the reaction of the corresponding alcohol with 1 in the presence of Et₃N (eq 3).



2d, R = methyl; **2e**, R = ethyl; **2f**, R = *tert*-butyl

(1) For examples of the use of matrix isolation techniques in silylene chemistry, see: (a) Drahnak, T. J.; Michl, J.; West, R. *J. Am. Chem. Soc.* 1979, 101, 5427. (b) Michalczyk, M. J.; Fink, M. J.; De Young, D. J.; Carlson, C. W.; Welsh, K. M.; West, R.; Michl, J. *Silicon, Germanium, Tin Lead Compd.* 1986, 9, 75. Sekiguchi, A.; Hagiwara, K.; Ando, W. *Chem. Lett.* 1987, 1, 209.

(2) Ishikawa, M.; Kumada, M. *J. Organomet. Chem.* 1972, 42, 325.

(3) Tan, R.; Yokelson, H. B.; Gillette, G. R.; West, R. *Inorg. Synth.*, in press. Chen, S.-M.; West, R. *Organometallic Syntheses*; Elsevier: Amsterdam, 1988; Vol. 4, pp 506-597.

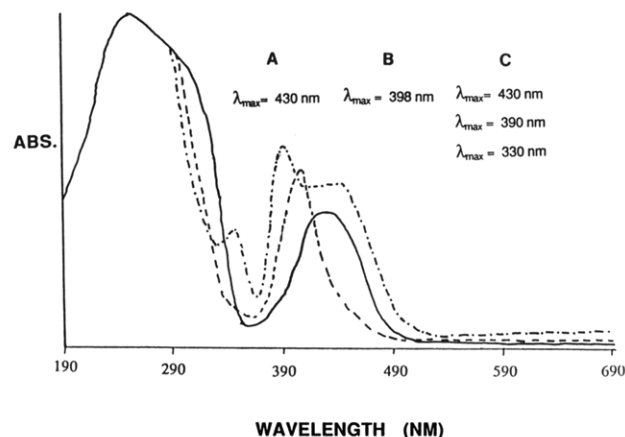
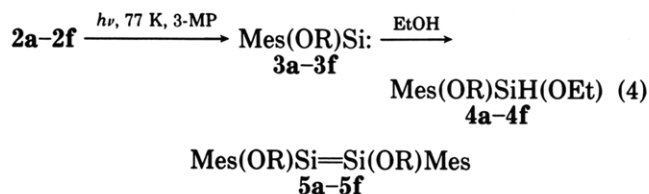


Figure 1. UV spectra of **3a** in 3-MP: (A) after 15-min irradiation at 77 K (—); (B) after annealing of the matrix (---); (C) after further warming of the matrix (-.-).

Photolysis of Oxy-Substituted Trisilanes at 77 K. Irradiation of frozen solutions of **2a–2f** in 3-methylpentane (3-MP) with 254-nm light produced colored matrices. The new absorptions are assigned to the $n \rightarrow p$ transition of the silylenes **3a–3f**. An electronic spectrum typical of these matrices is shown in Figure 1 for **3a**, and the absorption maxima for **3a–3f** are listed in Table I. The presence of **3a–3f** was confirmed by trapping experiments with ethanol (EtOH), leading to products having GC-MS spectra consistent with the ethanol adducts **4a–4f** (eq 4).



The range of λ_{max} values for the oxy-substituted silylenes **3a–3f** correlates well with the value (390 nm) predicted by theoretical calculations for H(OH)Si: by Apeloig and Karni.⁴ The presence of a π -donor substituent on the silylene is predicted to cause a substantial hypsochromic shift in the absorption maximum, attributed to a greater stabilization of the ground-state singlet than of the excited-state singlet.⁵ A good model compound for comparison is Mes(H)Si:, for which λ_{max} in a 3-MP matrix is 498 nm.^{1b}

Annealing of the 3-MP matrices containing **3c–3f** leads directly to formation of the unstable disilenes **5c–5f**, as reported for other silylenes.^{2b} For **3a** and **3b**, however, as the matrix annealed, the 430-nm band for the silylene diminished and a new band grew at 398 nm. When the compounds were warmed further, the band at 398 nm decayed and three bands due to the disilenes **5a** and **5b** grew in at 330, 390, and 430 nm. If the matrix was annealed and then quickly recooled to 77 K, the 398-nm band was stable and did not revert to the 430-nm band even under photolytic conditions. When EtOH was included in the matrix, the initial change was observed upon annealing but no new bands were seen upon further warming, and trapping products **4a** and **4b** were detected by GC-MS. These data are consistent with the assignment of both the 430- and 398-nm bands to the silylenes **2a** and **2b**.

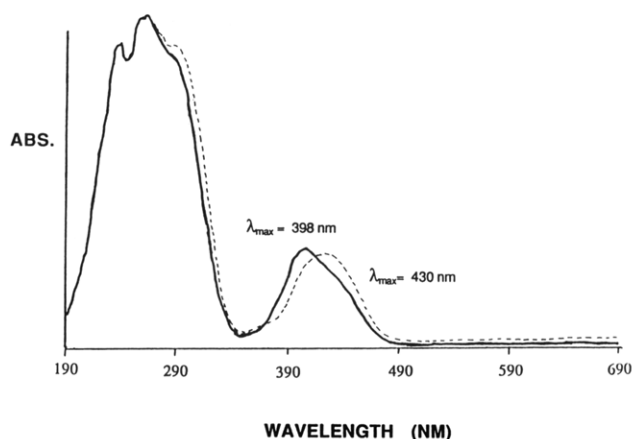


Figure 2. UV spectra of **3a** in 1:1 3-MP/isopentane: (a) after 15-min irradiation at 77 K (---); and (b) after 25 min at 77 K with no irradiation (—).

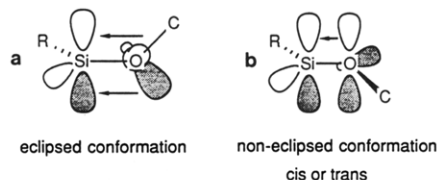


Figure 3. Two possible conformers of oxy-substituted silylenes: (a) eclipsed conformation; (b) noneclipsed conformation.

In order to investigate the effect of the matrix environment on the UV transition in oxy-substituted silylenes, trisilanes **2a–2f** were irradiated in a less viscous glass composed of a 1:1 (v/v) mixture of 3-MP/isopentane.⁶ For silylenes **3c–3f** no change in the initial λ_{max} value or in the annealing behavior was observed. For **3a** and **3b** only the shorter wavelength bands at 398 nm were observed after irradiation; annealing of the matrix led to disilene formation as before. The photolysis was also done at 77 K in a glass made of 4:1 (v/v) 3-MP/isopentane, with a viscosity intermediate between the two previously described. Irradiation of **2a** and **2b** at 77 K gave a colored matrix whose electronic spectrum was exactly the same as that observed for pure 3-MP. When the matrix stood at 77 K, the band at 430 nm shifted to 398 nm. The spectra for **3a** are shown in Figure 2. The species giving rise to the 398-nm band is stable in this matrix at 77 K, but when the matrix is annealed, the band decays and is replaced by the bands due to the disilene.

Two possible explanations for this behavior can be envisioned. The shift could be due to a triplet silylene that relaxes to a singlet silylene when the matrix is annealed. The changes could also be due to a nonrelaxed ground-state geometry of the silylene that assumes its minimum energy geometry as the glass softens.

The first of these possibilities, that the triplet silylene is formed initially, seems unlikely for two reasons. First, attempts to observe an ESR signal for **3a** in 3-MP at 77 K were unsuccessful. Second, theoretical calculations of singlet-triplet splittings in silylenes predict that π -donor ligands would stabilize the singlet by 15 kcal/mol with respect to the triplet, increasing the energy gap to approximately 36 kcal/mol.⁵

The second possibility, that the silylene is formed in a nonrelaxed geometry which relaxes to the equilibrium geometry as the restrictions of the matrix are lessened, appears to be a more likely explanation. If the silylene

(4) Apeloig, Y.; Karni, M. *J. Chem. Soc., Chem. Commun.* **1985**, 1048.

(5) Luke, B. T.; Pople, J. A.; Krogh-Jespersen, K. B.; Apeloig, Y.; Karni, M.; Chandrasekhar, J.; Schleyer, P. v. R. *J. Am. Chem. Soc.* **1986**, *108*, 270.

(6) Lombardi, J. R.; Raymond, J. W.; Albrecht, A. C. *J. Chem. Phys.* **1964**, *40*, 1148. The viscosities differ by 103×10^3 P at 77 K.

Table II. Summary of Crystal Data and Intensity Collection for 2c, 2a, and 6

	C ₂₁ H ₃₄ Si ₃ O	C ₂₇ H ₄₆ Si ₃ O	C ₆₃ H ₈₄ Si ₃ O ₃
empirical formula	C ₂₁ H ₃₄ Si ₃ O	C ₂₇ H ₄₆ Si ₃ O	C ₆₃ H ₈₄ Si ₃ O ₃
fw	386.52	470.38	972.92
cryst dimens, mm	0.4 × 0.4 × 0.5	0.5 × 0.5 × 0.6	0.3 × 0.4 × 0.4
temp, K	293	293	293
cell params			
<i>a</i> , Å	16.609 (3)	13.078 (2)	15.541 (2)
<i>b</i> , Å	18.081 (3)	12.054 (3)	17.708 (3)
<i>c</i> , Å	20.029 (3)	15.111 (3)	11.988 (2)
α, deg			109.70 (1)
β, deg		102.05 (1)	109.60 (1)
γ, deg			78.86 (1)
space group	<i>Pbca</i>	<i>P2₁/c</i>	<i>P1</i> (No. 2)
<i>Z</i>	8	4	2
calcd density, g/cm ³	1.04	1.12	1.11
abs coeff, μ, cm ⁻¹	1.56	2.04	1.3
Nicolet diffractometer	P3/F (Cu)	P1 (Mo)	P3/F (Mo)
scan type	θ-2θ	ω	θ-2θ
scan range below 2θ(Kα ₁) deg	1.0	1.0	0.9
scan range above 2θ(Kα ₂), deg	1.0	1.0	0.9
scan speed, deg/min	2.93-29.3	2.93-29.3	2.93-29.3
bkgd/scan ratio	profile anal.	profile anal.	profile anal.
2θ limits, deg	3.0-115.0	3.5-48.0	3.5-40.0
[(sin θ)/λ] _{max}	0.631	0.963	0.827
no. of unique data measd	4102	2896	5468
no. of data > 3σ	3629	2193	4751
<i>R</i> ^a	0.03	0.03	0.04
discrepancy indices			
<i>R</i> ₁	0.051	0.064	0.036
<i>R</i> ₂	0.056	0.076	0.031
goodness of fit	1.976	1.504	1.409
observn/variable ratio	11.4	8.67	7.98
final diff, ρ _{max} , e/Å ³	0.28	0.58	0.20

$$^a \text{Weight} = [\sigma^2(F) + p^2F^2]^{-1}.$$

were formed in a conformation such that the overlap between the empty p orbital at silicon and the lone-pair orbital of the oxygen atom was poor, the observed blue shift of the silylene relative to the signal for the unsubstituted model silylene would be attenuated somewhat. As this conformation relaxed to a geometry that increased the overlap between the orbitals in question, the UV maximum would then be blue-shifted, as observed.⁷⁻⁹

Two possible conformers of oxy-substituted silylenes are shown in Figure 3. The first depicts the silylene with the C-O bond of the oxy group eclipsed with the empty p orbital at silicon. In this conformation, stabilization of the silylene by oxygen donation would be minimized. Rotation about the Si-O bond by 90° would bring the lone-pair p orbital of oxygen into an eclipsed geometry with respect to the empty p orbital at Si, as is shown in Figure 3b. The increased overlap in this geometry would explain the observed blue shifts in the hindered (aryloxy)silylenes after annealing.¹⁰

To gain further insight into the origin of the UV spectral changes for (aryloxy)silylenes, the structures of two of the precursors, 2a and 2c, were determined by X-ray crystallography. Determination of the structures of the pre-

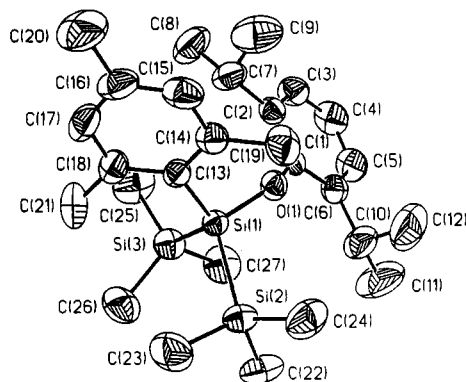


Figure 4. Thermal ellipsoid plot of 2a (50% probability ellipsoids). Hydrogen atoms are omitted for clarity.

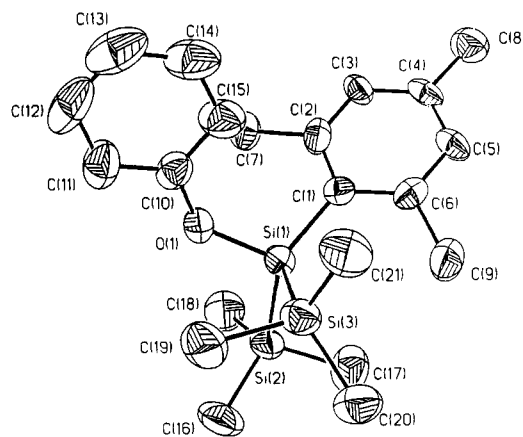


Figure 5. Thermal ellipsoid plot of 2c (50% probability ellipsoids). Hydrogen atoms are omitted for clarity.

(7) Oxy-substituted carbenes are known to exist as cis-trans isomers with distinct properties. See: Kesselmayr, M. A.; Sheridan, R. S. *J. Am. Chem. Soc.* **1986**, *108*, 844. Other examples of geometrical isomerism in carbenes have also been reported.⁸

(8) (a) Trozzolo, A. M.; Wasserman, E.; Yager, W. *J. Am. Chem. Soc.* **1965**, *87*, 129. (b) Hutton, R. S.; Manion, M. L.; Roth, H. D.; Wasserman, E. *J. Am. Chem. Soc.* **1974**, *96*, 4680. (c) Hutton, R. S.; Roth, H. D. *J. Am. Chem. Soc.* **1978**, *100*, 4324. (d) Murai, H.; Torres, M.; Strausz, O. P. *J. Am. Chem. Soc.* **1980**, *102*, 1421. (e) Murai, H.; Torres, M.; Strausz, O. P. *Chem. Phys. Lett.* **1980**, *70*, 358. (f) Hutton, R. S.; Roth, H. D.; Manion-Shilling, M. L.; Suggs, J. W. *J. Am. Chem. Soc.* **1981**, *103*, 5147.

(9) For an example of a similar matrix effect on the geometry of a carbene, see: Nazran, A. S.; Gabe, E. J.; LePage, Y.; Northcott, D. J.; Park, J. M.; Griller, D. *J. Am. Chem. Soc.* **1986**, *108*, 2912.

(10) Apeloig, Y. *Theoretical Aspects of Organosilicon Compounds*. In *The Chemistry of Organic Silicon Compounds*; Patai, S., Rappoport, Z., Eds.; Wiley: New York, 1989; pp 169-175.

cursors should give an indication of the geometry of the silylene as it is first formed, assuming no rearrangement upon photolysis.

Table III. Bond Lengths (Å) and Bond Angles (deg) for 2a

Si(1)-Si(2)	2.371 (1)	Si(1)-Si(3)	2.393 (1)
Si(1)-O(1)	1.668 (2)	Si(1)-C(13)	1.911 (3)
Si(2)-C(22)	1.882 (5)	Si(2)-C(23)	1.859 (4)
Si(2)-C(24)	1.874 (5)	Si(3)-C(25)	1.873 (5)
Si(3)-C(26)	1.882 (5)	Si(3)-C(27)	1.869 (5)
O(1)-C(1)	1.375 (4)	C(1)-C(2)	1.384 (5)
C(1)-C(6)	1.398 (5)	C(2)-C(3)	1.394 (5)
C(2)-C(7)	1.525 (5)	C(3)-C(4)	1.369 (6)
C(4)-C(5)	1.365 (6)	C(5)-C(6)	1.394 (5)
C(6)-C(10)	1.513 (6)	C(7)-C(8)	1.539 (6)
C(7)-C(9)	1.492 (7)	C(10)-C(11)	1.531 (8)
C(10)-C(12)	1.535 (8)	C(13)-C(14)	1.404 (5)
C(13)-C(18)	1.407 (5)	C(14)-C(15)	1.397 (6)
C(14)-C(19)	1.522 (6)	C(15)-C(16)	1.366 (6)
C(16)-C(17)	1.370 (7)	C(16)-C(20)	1.526 (8)
C(17)-C(18)	1.388 (6)	C(18)-C(21)	1.518 (6)
Si(2)-Si(1)-Si(3)	105.9 (1)	Si(2)-Si(1)-O(1)	110.8 (1)
Si(3)-Si(1)-O(1)	106.6 (1)	Si(2)-Si(1)-C(13)	107.9 (1)
Si(3)-Si(1)-C(13)	121.0 (1)	O(1)-Si(1)-C(13)	104.6 (1)
Si(1)-Si(2)-C(22)	111.6 (2)	Si(1)-Si(2)-C(23)	107.8 (2)
Si(1)-Si(2)-C(24)	114.4 (2)	Si(1)-Si(3)-C(25)	115.5 (2)
Si(1)-Si(3)-C(26)	111.9 (2)	Si(1)-Si(3)-C(27)	107.7 (1)
Si(1)-O(1)-C(1)	136.6 (2)	O(1)-C(1)-C(2)	120.6 (3)
O(1)-C(1)-C(6)	117.5 (3)	C(2)-C(1)-C(6)	121.8 (3)
C(1)-C(2)-C(3)	117.9 (3)	C(1)-C(2)-C(7)	122.1 (3)
C(3)-C(2)-C(7)	119.8 (3)	C(2)-C(3)-C(4)	121.3 (4)
C(3)-C(4)-C(5)	119.9 (4)	C(4)-C(5)-C(6)	121.5 (4)
C(1)-C(6)-C(5)	117.5 (3)	C(1)-C(6)-C(10)	120.0 (3)
C(5)-C(6)-C(10)	122.4 (4)	C(2)-C(7)-C(8)	113.2 (4)
C(2)-C(7)-C(9)	110.2 (4)	C(6)-C(10)-C(11)	113.1 (4)
C(6)-C(10)-C(12)	109.3 (4)	Si(1)-C(13)-C(14)	120.3 (2)
Si(1)-C(13)-C(18)	122.8 (3)	C(14)-C(13)-C(18)	116.9 (3)
C(13)-C(14)-C(15)	120.0 (3)	C(13)-C(14)-C(19)	123.8 (3)
C(15)-C(14)-C(19)	116.2 (3)	C(14)-C(15)-C(16)	122.4 (4)
C(15)-C(16)-C(17)	117.9 (4)	C(15)-C(16)-C(20)	121.1 (4)
C(17)-C(16)-C(20)	121.0 (4)	C(16)-C(17)-C(18)	121.8 (4)
C(13)-C(18)-C(17)	120.7 (3)	C(13)-C(18)-C(21)	122.2 (3)
C(17)-C(18)-C(21)	117.1 (3)		

Table IV. Bond Lengths (Å) and Bond Angles (deg) for 2c

Si(1)-Si(2)	2.355 (2)	Si(1)-Si(3)	2.378 (2)
Si(1)-O(1)	1.694 (3)	Si(1)-C(1)	1.894 (5)
Si(2)-C(16)	1.861 (6)	Si(2)-C(17)	1.863 (7)
Si(2)-C(18)	1.851 (5)	Si(3)-C(19)	1.858 (7)
Si(3)-C(20)	1.884 (5)	Si(3)-C(21)	1.875 (6)
O(1)-C(10)	1.372 (5)	C(1)-C(2)	1.423 (6)
C(1)-C(6)	1.408 (7)	C(2)-C(3)	1.376 (8)
C(2)-C(7)	1.575 (7)	C(3)-C(4)	1.394 (7)
C(4)-C(5)	1.383 (6)	C(4)-C(8)	1.497 (8)
C(5)-C(6)	1.386 (8)	C(6)-C(9)	1.576 (7)
C(10)-C(11)	1.363 (8)	C(10)-C(15)	1.398 (8)
C(11)-C(12)	1.392 (8)	C(12)-C(13)	1.369 (11)
C(13)-C(14)	1.353 (10)	C(14)-C(15)	1.377 (8)
Si(2)-Si(1)-Si(3)	109.7 (1)	Si(2)-Si(1)-O(1)	104.2 (1)
Si(3)-Si(1)-O(1)	101.8 (1)	Si(2)-Si(1)-C(1)	109.5 (1)
Si(3)-Si(1)-C(1)	120.2 (1)	O(1)-Si(1)-C(1)	110.1 (2)
Si(1)-Si(2)-C(16)	112.0 (2)	Si(1)-Si(2)-C(17)	107.5 (2)
Si(1)-Si(2)-C(18)	111.5 (2)	Si(1)-Si(3)-C(19)	103.9 (2)
Si(1)-Si(3)-C(20)	113.3 (2)	Si(1)-Si(3)-C(21)	115.6 (2)
Si(1)-O(1)-C(10)	127.8 (3)	Si(1)-C(1)-C(2)	123.9 (4)
Si(1)-C(1)-C(6)	122.1 (3)	C(2)-C(1)-C(6)	113.9 (4)
C(1)-C(2)-C(3)	123.8 (4)	C(1)-C(2)-C(7)	121.3 (5)
C(3)-C(2)-C(7)	114.9 (4)	C(2)-H(2)-C(7)	170.6 (7)
C(2)-C(3)-C(4)	119.2 (4)	C(3)-C(4)-C(5)	119.7 (5)
C(3)-C(4)-C(8)	120.3 (4)	C(5)-C(4)-C(8)	119.9 (5)
C(4)-C(5)-C(6)	119.9 (5)	C(1)-C(6)-C(5)	123.3 (4)
C(1)-C(6)-C(9)	120.0 (5)	C(5)-C(6)-C(9)	116.7 (4)
C(6)-H(6)-C(9)	174.6 (7)	O(1)-C(10)-C(11)	117.5 (5)
O(1)-C(10)-C(15)	121.9 (5)	C(11)-C(10)-C(15)	120.5 (5)
C(10)-C(11)-C(12)	119.3 (6)	C(11)-C(12)-C(13)	120.8 (7)
C(12)-C(13)-C(14)	119.0 (6)	C(13)-C(14)-C(15)	122.5 (6)
C(10)-C(15)-C(14)	118.0 (6)		

X-ray Crystallography of 2a and 2c. Crystals of both compounds suitable for X-ray analysis were grown from hexane at room temperature. Both structures were solved

Table V. Atomic Coordinates ($\times 10^4$) and Equivalent Isotropic Displacement Parameters ($\text{Å}^2 \times 10^3$) for 2a

	x	y	z	$U(\text{eq})^a$
Si(1)	6567 (1)	3379 (1)	1471 (1)	37 (1)
Si(2)	6571 (1)	4204 (1)	2391 (1)	53 (1)
Si(3)	5185 (1)	3234 (1)	1160 (1)	55 (1)
O(1)	6895 (1)	2545 (1)	1700 (1)	45 (1)
C(1)	6612 (2)	1831 (2)	1666 (2)	40 (1)
C(2)	6640 (2)	1442 (2)	1070 (2)	46 (1)
C(3)	6373 (2)	711 (2)	1073 (2)	60 (1)
C(4)	6085 (3)	387 (2)	1643 (2)	69 (2)
C(5)	6076 (3)	775 (2)	2227 (2)	67 (2)
C(6)	6343 (2)	1505 (2)	2258 (2)	52 (1)
C(7)	7014 (3)	1766 (2)	439 (2)	68 (2)
C(8)	6617 (4)	1483 (3)	-206 (2)	103 (2)
C(9)	7898 (3)	1620 (3)	429 (3)	109 (3)
C(10)	6399 (3)	1927 (2)	2909 (2)	79 (2)
C(11)	5743 (5)	1710 (4)	3409 (3)	136 (3)
C(12)	7250 (4)	1844 (4)	3197 (3)	121 (3)
C(13)	7349 (2)	3720 (2)	842 (2)	39 (1)
C(14)	8168 (2)	3555 (2)	933 (2)	47 (1)
C(15)	8726 (3)	3749 (2)	442 (2)	62 (2)
C(16)	8513 (3)	4119 (2)	-125 (2)	67 (2)
C(17)	7722 (3)	4318 (2)	-199 (2)	62 (2)
C(18)	7144 (2)	4140 (2)	276 (2)	49 (1)
C(19)	8505 (2)	3182 (2)	1554 (2)	64 (2)
C(20)	9138 (4)	4321 (3)	-653 (3)	108 (3)
C(21)	6298 (3)	4431 (3)	161 (2)	75 (2)
C(22)	5687 (3)	4037 (3)	2960 (2)	80 (2)
C(23)	6499 (3)	5161 (2)	2057 (3)	86 (2)
C(24)	7491 (3)	4146 (3)	2929 (2)	80 (2)
C(25)	5007 (3)	2796 (3)	325 (3)	94 (2)
C(26)	4619 (3)	4134 (3)	1202 (3)	86 (2)
C(27)	4701 (3)	2610 (3)	1787 (3)	82 (2)

^a Equivalent isotropic U defined as one-third of the trace of the orthogonalized U_{ij} tensor.

Table VI. Atomic Coordinates ($\times 10^4$) and Equivalent Isotropic Displacement Parameters ($\text{Å}^2 \times 10^3$) for 2c

	x	y	z	$U(\text{eq})^a$
Si(1)	2297 (1)	2992 (1)	861 (1)	42 (1)
Si(2)	2140 (1)	4524 (1)	-125 (1)	52 (1)
Si(3)	3814 (1)	3198 (1)	2029 (1)	53 (1)
O(1)	2646 (3)	1931 (2)	251 (2)	49 (1)
C(1)	984 (4)	2693 (3)	1153 (3)	40 (2)
C(2)	207 (4)	2000 (3)	627 (3)	46 (2)
C(3)	-728 (4)	1748 (4)	861 (3)	45 (2)
C(4)	-961 (4)	2220 (4)	1637 (3)	43 (2)
C(5)	-264 (4)	2952 (4)	2148 (3)	45 (2)
C(6)	679 (4)	3179 (3)	1905 (3)	43 (2)
C(7)	353 (5)	1493 (5)	-299 (3)	65 (2)
C(8)	-1987 (4)	1988 (4)	1890 (4)	63 (2)
C(9)	1415 (4)	4048 (5)	2505 (4)	69 (2)
C(10)	2881 (4)	860 (4)	529 (3)	51 (2)
C(11)	3438 (4)	239 (4)	41 (4)	68 (2)
C(12)	3674 (5)	-859 (5)	289 (6)	89 (3)
C(13)	3338 (5)	-1323 (5)	1005 (4)	89 (3)
C(14)	2793 (5)	-690 (5)	1484 (5)	79 (3)
C(15)	2550 (4)	403 (4)	1272 (4)	67 (2)
C(16)	3436 (4)	5013 (5)	-294 (4)	78 (3)
C(17)	1522 (5)	5673 (4)	401 (4)	84 (3)
C(18)	1323 (5)	4189 (5)	-1248 (4)	75 (3)
C(19)	4899 (4)	2742 (5)	1493 (4)	75 (3)
C(20)	4089 (5)	4682 (4)	2394 (4)	71 (2)
C(21)	3852 (5)	2323 (5)	3061 (4)	72 (2)

^a Equivalent isotropic U defined as one-third of the trace of the orthogonalized U_{ij} tensor.

by direct methods and refined by blocked-cascade least-squares refinement for data with $F_o > 3\sigma(F\#o)$.¹¹ The experimental details for the structures are given in Table II. Bond lengths and angles for 2a are given in Table III; those for 2c are given in Table IV. Atomic coordinates

(11) SHELXTL; Nicolet X-Ray Instruments: Madison, WI, 1985.

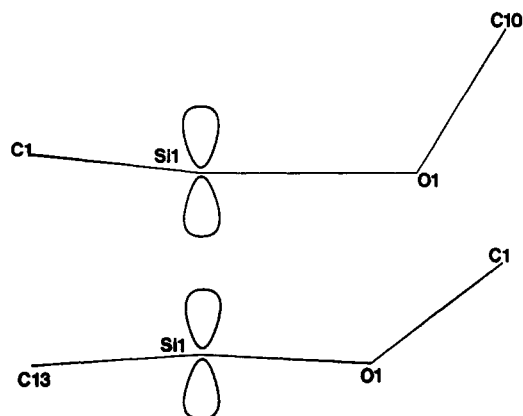


Figure 6. Structures of incipient silylenes **3a** (below) and **3c** (above), based on X-ray structural data for **2a** and **2c**. This view shows the C-Si-O plane coming out of the page. The dihedral angles C-O-Si-(p orbital) are 24.2° for **2a** and 28.6° for **2c**.

for **2a** are shown in Table V, and those for **2c** are given in Table VII.

A thermal ellipsoid plot of **2a** is shown in Figure 4 and for **2c** in Figure 5. The structures of **2a** and **2c** are similar to several recently published trisilane structures,¹² the bond lengths about the central silicon atom are all in the range of normal values for Si-O, Si-C, and Si-Si bonds.¹³ The Si-Si-Si bond angles of 106° in **2a** and 109.7° in **2c** are slightly smaller than those of the previously published trisilanes (114–118°).¹² The Si-O-C bond angles, 136.3° in **2a** and 127.8° in **2c**, are larger than the usual angles found in silyl ethers.¹⁴

The structural features of **2a** and **2c** most pertinent to the UV transitions in oxy-substituted silylenes are the dihedral angles C-Si-O-C. These angles show the initial orientation of the C-O bond with respect to the empty p orbital of the silylene after the two trimethyl groups are removed. The structures of the incipient silylenes are shown in Figure 6. The dihedral angle in **3a** is 118.6° and in **3c** is 65.8°. Thus for both silylenes, assuming no rearrangement is possible following loss of the two trimethylsilyl groups, the C-O bond of the oxy group is nearly eclipsed with the empty p orbital at silicon, decreasing the overlap and reducing the blue shift due to π -donation.

The structures of **2a** and **2c** raise the question of why **3c** never shows a long-wavelength band although it is presumably formed in an eclipsed conformation. The probable explanation is that in the most rigid matrix employed in these studies, 3-MP, **3a** is too bulky to be conformationally mobile at 77 K while **3c** is free to rotate to the lower energy conformation.

Solution Photolysis of 2a. We attempted to synthesize a stable oxy-substituted disilene by irradiating **2a** with 254-nm light at -60 °C in pentane in a known synthetic route to stable disilenes.¹⁵ When a sample of **2a** was irradiated for 20 h at -60 °C, a bright yellow solution was formed. As the solution was warmed to room temperature,

(12) (a) Weidenbruch, M.; Flintjer, B.; Peters, K.; von Schnering, H. G. *Angew. Chem., Int. Ed. Engl.* 1986, 25, 1129. (b) Weidenbruch, M.; Flintjer, B.; Kramer, K.; Peters, K.; von Schnering, H. G. *J. Organomet. Chem.* 1988, 340, 13. (c) Fink, M. J.; Puranik, D. B. *Organometallics* 1986, 5, 1809. (d) Corey, J. Y.; Chang, L. S.; Corey, E. R. *Organometallics* 1987, 6, 1595.

(13) Armitage, D. A. In *Comprehensive Organometallic Chemistry*; Wilkinson, G., Stone, F. G. A., Abel, E. W., Eds.; Pergamon: New York, 1982; Vol 2.

(14) Bordeau, M.; Dedier, J.; Frainnet, E.; Fayet, J.-P.; Mauret, P. J. *Organomet. Chem.* 1973, 61, 91. Bordeau, M.; Dedier, J.; Frainnet, E.; Fayet, J.-P.; Mauret, J. *J. Organomet. Chem.* 1973, 59, 125.

(15) West, R. *Angew. Chem., Int. Ed. Engl.* 1987, 26, 1201–1211.

Table VII. Bond Lengths (Å) for 6^a

Si(1)-Si(2)	2.407 (2)	Si(1)-Si(3)	2.380 (1)
Si(1)-O(1)	1.662 (2)	Si(1)-C(1)	1.887 (3)
Si(2)-Si(3)	2.342 (1)	Si(2)-O(2)	1.647 (2)
Si(2)-C(19)	1.884 (2)	Si(3)-O(3)	1.660 (2)
Si(3)-C(10)	1.898 (2)	O(1)-C(28)	1.388 (3)
O(2)-C(41)	1.392 (4)	O(3)-C(53)	1.392 (3)
C(1)-C(2)	1.408 (4)	C(1)-C(6)	1.405 (5)
C(2)-C(3)	1.387 (4)	C(2)-C(9)	1.500 (5)
C(3)-C(4)	1.381 (6)	C(4)-C(5)	1.368 (5)
C(4)-C(8)	1.522 (5)	C(5)-C(6)	1.398 (4)
C(6)-C(7)	1.509 (4)	C(10)-C(11)	1.421 (4)
C(10)-C(15)	1.404 (4)	C(11)-C(12)	1.392 (4)
C(11)-C(18)	1.503 (5)	C(12)-C(13)	1.369 (6)
C(13)-C(14)	1.375 (6)	C(13)-C(17)	1.518 (5)
C(14)-C(15)	1.393 (4)	C(15)-C(16)	1.501 (5)
C(19)-C(20)	1.416 (3)	C(19)-C(23)	1.413 (3)
C(20)-C(21)	1.391 (3)	C(20)-C(27)	1.501 (3)
C(21)-C(22)	1.380 (4)	C(22)-C(24)	1.379 (3)
C(22)-C(26)	1.519 (4)	C(23)-C(24)	1.396 (3)
C(23)-C(25)	1.497 (3)	C(28)-C(29)	1.406 (3)
C(28)-C(34)	1.397 (3)	C(29)-C(30)	1.377 (3)
C(29)-C(38)	1.518 (3)	C(30)-C(32)	1.376 (4)
C(32)-C(33)	1.370 (4)	C(33)-C(34)	1.399 (3)
C(34)-C(35)	1.507 (3)	C(35)-C(36)	1.533 (4)
C(35)-C(37)	1.520 (6)	C(28)-C(39)	1.526 (4)
C(38)-C(40)	1.526 (5)	C(41)-C(42)	1.410 (3)
C(41)-C(46)	1.395 (4)	C(42)-C(43)	1.386 (5)
C(42)-C(50)	1.510 (4)	C(43)-C(44)	1.365 (5)
C(44)-C(45)	1.372 (4)	C(45)-C(46)	1.396 (5)
C(46)-C(47)	1.511 (3)	C(47)-C(48)	1.528 (4)
C(47)-C(49)	1.528 (4)	C(50)-C(51)	1.502 (4)
C(50)-C(52)	1.526 (4)	C(53)-C(54)	1.390 (4)
C(53)-C(58)	1.395 (5)	C(54)-C(55)	1.393 (4)
C(54)-C(62)	1.513 (5)	C(55)-C(56)	1.366 (6)
C(56)-C(57)	1.367 (5)	C(57)-C(58)	1.396 (4)
C(58)-C(59)	1.510 (4)	C(59)-C(60)	1.516 (4)
C(59)-C(61)	1.528 (6)	C(62)-C(63)	1.490 (6)
C(62)-C(64)	1.495 (5)		

^a Estimated standard deviations are given in parentheses.

a distinct deepening of the color of the solution was noted. The solvent was removed in vacuo, and the residue was redissolved in C₆D₆. Analysis of the solution by ²⁹Si NMR spectroscopy showed that one new product was formed with a ²⁹Si resonance at +7.33 ppm. The photolysis was very inefficient; in contrast to disilene precursors previously studied, much starting material remained after irradiation. The mixture was chromatographed on silica gel (hexane), and two bands were collected. The first fraction was recovered starting material, while the second fraction contained only the compound with the resonance at +7.33 ppm in the ²⁹Si NMR spectrum. Recrystallization from hexane yielded an air-stable yellow crystalline solid whose analytical data did not provide unambiguous structural assignment. In order to determine the structure of this compound, an X-ray crystal structure analysis was undertaken.

Suitable crystals for X-ray analysis were grown from hexane at room temperature, and the structure was solved in the same manner as described above. The experimental details for the structures are given in Table II. Bond lengths and angles are given in Tables VII and VIII, and atomic coordinates are shown in Table IX.

The structure was determined to be the cyclotrisilane **6**, the first heteroatom-substituted cyclotrisilane. An ORTEP plot of **6** is shown in Figure 7. The cis-trans geometry of **6** is identical with that found for [(mes)(*t*-Bu)Si]₃.¹⁶ The Si-Si bond lengths in the ring range from 2.34 to 2.41 Å and are typical for cyclotrisilanes.¹⁷ The exocyclic Si-O

(16) Dewan, J. C.; Murakami, S.; Snow, J. T.; Collins, S.; Masamune, S. *J. Chem. Soc., Chem. Commun.* 1985, 892.

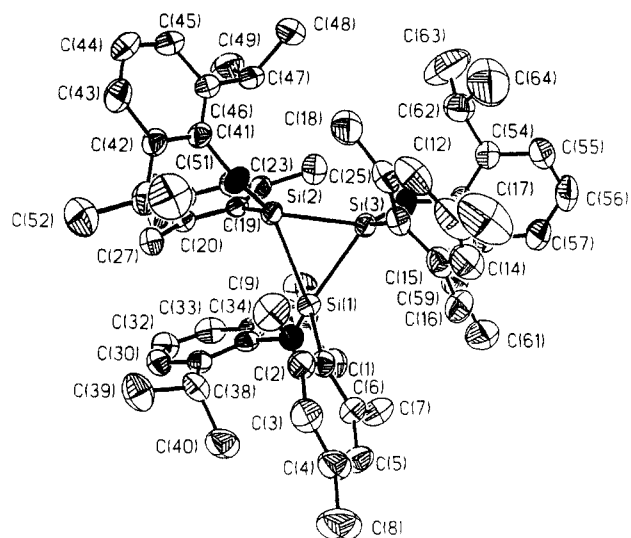


Figure 7. Thermal ellipsoid plot for **6** (50% probability ellipsoids). Hydrogen atoms and some atom labels are omitted for clarity. The oxygen atoms are indicated by solid ellipsoids.

and Si-C bond lengths are also normal for organosilanes.

The solution of the structure of **6** allowed the rationalization of several interesting spectroscopic properties of the molecule. Although only one ^{29}Si NMR signal is observed in solution at low resolution, if high-resolution techniques including restriction acquisition, Gaussian multiplication, and zero filling are employed, two peaks can be resolved with chemical shifts of +7.34 and +7.32 ppm, reflecting the asymmetry of the molecule. The ^1H NMR spectrum shows an interesting pattern in the isopropyl methyl region. Three distinct resonances are observed that are integrated in a 1:1:1 ratio. The most upfield resonance is very broad and is probably due to the aryloxy group which is on the same side of the ring as the two mesityl groups, broadened due to hindered rotation about the C-O bond. The other two resonances result from the different environment for each of the two aryloxy groups on the same side of the ring, which are forced to bend away from one another to avoid severe steric repulsions.

The UV absorption maxima for **6** in hexane are 298, 353, and 380 nm. The 380-nm band represents a very long wavelength absorption for a cyclotrisilane; only in *cis*-[(Mes)(*t*-Bu)Si] $_3$ is a longer wavelength absorption reported.¹⁸ The low-energy transition in **6** probably reflects the perturbation of the silicon σ framework by the lone-pair electrons of the pendant oxygen atoms.

Since cyclotrisilanes are photochemical precursors to disilenes, **6** was irradiated in both solution and hydrocarbon glass in an effort to observe the disilene. Photolysis of a solution of **6** in cyclohexane- d_{12} gave no evidence for disilene by ^{29}Si NMR spectroscopy. New products containing Si-H resonances were detected by ^1H NMR spectroscopy. This would indicate that bond homolysis to yield silyl radicals occurred instead of the expected fragmentation to silylene and disilene. When **6** was irra-

Table VIII. Bond Angles (deg) for **6**^a

Si(2)-Si(1)-Si(3)	58.6 (1)	Si(2)-Si(1)-O(1)	110.7 (1)
Si(3)-Si(1)-O(1)	124.5 (1)	Si(2)-Si(1)-C(1)	136.9 (1)
Si(3)-Si(1)-C(1)	117.2 (1)	O(1)-Si(1)-C(1)	105.0 (1)
Si(1)-Si(2)-Si(3)	60.1 (1)	Si(1)-Si(2)-O(2)	127.1 (1)
Si(3)-Si(2)-O(2)	122.7 (1)	Si(1)-Si(2)-C(19)	107.0 (1)
Si(3)-Si(2)-C(19)	120.8 (1)	O(2)-Si(2)-C(19)	110.4 (1)
Si(1)-Si(3)-Si(2)	61.3 (1)	Si(1)-Si(3)-O(3)	131.7 (1)
Si(2)-Si(3)-O(3)	125.7 (1)	Si(1)-Si(3)-C(10)	105.2 (1)
Si(2)-Si(3)-C(10)	113.3 (1)	O(3)-Si(3)-C(10)	111.0 (1)
Si(1)-O(1)-C(28)	135.6 (2)	Si(2)-O(2)-C(41)	140.4 (1)
Si(3)-O(3)-C(53)	132.1 (1)	Si(1)-C(1)-C(2)	122.9 (2)
Si(1)-C(1)-C(6)	119.1 (2)	C(2)-C(1)-C(6)	117.9 (2)
C(1)-C(2)-C(3)	120.2 (3)	C(1)-C(2)-C(9)	121.7 (3)
C(3)-C(2)-C(9)	118.1 (3)	C(2)-C(3)-C(4)	121.8 (3)
C(3)-C(4)-C(5)	117.9 (3)	C(3)-C(4)-C(8)	121.7 (3)
C(5)-C(4)-C(8)	120.4 (4)	C(4)-C(5)-C(6)	122.4 (4)
C(1)-C(6)-C(5)	119.5 (3)	C(1)-C(6)-C(7)	123.0 (3)
C(5)-C(6)-C(7)	117.5 (3)	Si(3)-C(10)-C(11)	123.2 (2)
Si(3)-C(10)-C(15)	119.4 (2)	C(11)-C(10)-C(15)	117.4 (2)
C(10)-C(11)-C(12)	119.6 (3)	C(10)-C(11)-C(18)	123.6 (2)
C(12)-C(11)-C(18)	116.8 (3)	C(11)-C(12)-C(13)	122.8 (3)
C(12)-C(13)-C(14)	117.6 (3)	C(12)-C(13)-C(17)	120.9 (4)
C(14)-C(13)-C(17)	121.5 (4)	C(13)-C(14)-C(15)	122.3 (3)
C(10)-C(15)-C(14)	120.3 (3)	C(10)-C(15)-C(16)	122.8 (2)
C(14)-C(15)-C(16)	116.9 (3)	Si(2)-C(19)-C(20)	117.4 (2)
Si(2)-C(19)-C(23)	124.7 (2)	C(20)-C(19)-C(23)	117.8 (2)
C(19)-C(20)-C(21)	119.9 (2)	C(19)-C(20)-C(27)	123.0 (2)
C(21)-C(20)-C(27)	117.1 (2)	C(20)-C(21)-C(22)	122.3 (2)
C(21)-C(22)-C(24)	118.0 (2)	C(21)-C(22)-C(26)	120.5 (2)
C(24)-C(22)-C(26)	121.5 (2)	C(19)-C(23)-C(24)	119.9 (2)
C(19)-C(23)-C(25)	123.0 (2)	C(24)-C(23)-C(25)	117.1 (2)
C(22)-C(24)-C(23)	122.2 (2)	O(1)-C(28)-C(29)	120.6 (2)
O(1)-C(28)-C(34)	116.4 (2)	C(29)-C(28)-C(34)	122.8 (2)
C(28)-C(29)-C(30)	117.0 (2)	C(28)-C(29)-C(38)	120.7 (2)
C(30)-C(29)-C(38)	122.1 (2)	C(29)-C(30)-C(32)	122.0 (2)
C(30)-C(32)-C(33)	119.6 (2)	C(32)-C(33)-C(34)	122.0 (2)
C(28)-C(34)-C(33)	116.3 (2)	C(28)-C(34)-C(35)	120.7 (2)
C(33)-C(34)-C(35)	122.9 (2)	C(34)-C(35)-C(36)	114.2 (2)
C(34)-C(35)-C(37)	109.7 (2)	C(29)-C(38)-C(39)	114.3 (2)
C(29)-C(38)-C(40)	110.3 (2)	O(2)-C(41)-C(42)	115.5 (2)
O(2)-C(41)-C(46)	122.3 (2)	C(42)-C(41)-C(46)	122.1 (3)
C(41)-C(42)-C(43)	117.2 (3)	C(41)-C(42)-C(50)	122.2 (3)
C(43)-C(42)-C(50)	120.5 (2)	C(42)-C(43)-C(44)	122.0 (3)
C(43)-C(44)-C(45)	119.6 (4)	C(44)-C(45)-C(46)	122.0 (3)
C(41)-C(46)-C(45)	117.0 (2)	C(41)-C(46)-C(47)	125.4 (3)
C(45)-C(46)-C(47)	117.6 (3)	C(45)-C(47)-C(48)	112.6 (2)
C(46)-C(47)-C(49)	111.5 (2)	C(42)-C(50)-C(51)	112.2 (2)
C(42)-C(50)-C(52)	112.5 (3)	O(3)-C(53)-C(54)	119.2 (3)
O(3)-C(53)-C(58)	118.0 (2)	C(54)-C(53)-C(58)	122.7 (2)
C(53)-C(54)-C(55)	117.3 (3)	C(53)-C(54)-C(62)	122.2 (2)
C(55)-C(54)-C(62)	120.4 (3)	C(54)-C(55)-C(56)	121.7 (3)
C(55)-C(56)-C(57)	119.6 (3)	C(56)-C(57)-C(58)	122.1 (4)
C(53)-C(58)-C(57)	116.6 (3)	C(53)-C(58)-C(59)	121.9 (2)
C(57)-C(58)-C(59)	121.4 (3)	C(58)-C(59)-C(60)	110.2 (3)
C(58)-C(59)-C(61)	113.5 (2)	C(54)-C(62)-C(63)	110.7 (3)
C(54)-C(62)-C(64)	113.7 (3)		

^a Estimated standard deviations are given in parentheses.

diated in a 3-MP or isopentane glass with either visible or UV (254-nm) light, no reaction occurred.

An interesting feature of **6** is that it is not possible to make it by the usual methods of cyclotrisilane synthesis. The previously known three-membered rings have all been made by reduction of the dichlorosilane with alkali-metal naphthalenides.¹⁷ Attempts to make **6** via these routes were unsuccessful because the oxy substituent was not stable under the conditions of alkali-metal reduction. The photolytic method employed here represents a novel, albeit fortuitous, route to strained organosilicon compounds.

The mechanism of formation of **6** from **2a** under our conditions remains unclear. The two most probable pathways are represented in Figure 8. The first step in the reaction is known to be silylene extrusion; the silylene formed would most likely react with another silylene to form disilene **5a**. At this point either the unstable disilene

(17) For other examples of X-ray structures of cyclotrisilanes, see: (a) Matsumoto, H.; Sakamoto, A.; Nagai, Y. *J. Chem. Soc., Chem. Commun.* **1986**, 1768. (b) Watanabe, H.; Okawa, T.; Kato, M.; Nagai, Y. *J. Chem. Soc., Chem. Commun.* **1983**, 781. (c) Masamune, S.; Tobita, H.; Murakami, S. *J. Am. Chem. Soc.* **1983**, *105*, 6524. (d) Watanabe, H.; Kato, M.; Okawa, T.; Nagai, Y.; Goto, M. *J. Organomet. Chem.* **1984**, *271*, 225. (e) Watanabe, H.; Kougo, Y.; Kato, M.; Kuwabara, H.; Okawa, T.; Nagai, Y. *Bull. Chem. Soc. Jpn.* **1984**, *57*, 3019. (f) Schafer, A.; Weidenbruch, M.; Peters, K.; von Schnering, H.-G. *Angew. Chem., Int. Ed. Engl.* **1984**, *23*, 302. (g) Weidenbruch, M.; Thom, K.-L.; Pohl, S.; Saak, W. *J. Organomet. Chem.* **1987**, *329*, 151.

(18) Murakami, S.; Collins, S.; Masamune, S. *Tetrahedron Lett.* **1984**, *25*, 2131.

Table IX. Atomic Coordinates ($\times 10^4$) and Equivalent Isotropic Displacement Parameters ($\text{\AA}^2 \times 10^3$) for 6

	x	y	z	U(eq) ^a		x	y	z	U(eq) ^a
Si(1)	7664 (1)	2202 (1)	1512 (1)	34 (1)	C(30)	8776 (2)	4304 (2)	5252 (2)	46 (1)
Si(2)	7942 (1)	2974 (1)	375 (1)	33 (1)	C(32)	8139 (2)	4961 (2)	5378 (3)	54 (1)
Si(3)	6781 (1)	2096 (1)	-576 (1)	34 (1)	C(33)	7243 (2)	4881 (2)	4677 (3)	53 (1)
O(2)	8840 (1)	2858 (1)	-122 (1)	39 (1)	C(34)	6956 (2)	4156 (2)	3792 (2)	41 (1)
O(3)	5680 (1)	2350 (1)	-1199 (2)	42 (1)	C(35)	5964 (2)	4032 (2)	3091 (2)	50 (1)
C(1)	8163 (2)	1232 (1)	1908 (2)	39 (1)	C(36)	5345 (2)	4813 (2)	3033 (3)	75 (2)
C(2)	9004 (2)	829 (2)	1736 (2)	44 (1)	C(37)	5596 (2)	3558 (2)	3654 (3)	70 (2)
C(3)	9405 (2)	189 (2)	2214 (3)	56 (1)	C(38)	9222 (2)	2820 (2)	4364 (2)	48 (1)
C(4)	8993 (2)	-81 (2)	2849 (3)	61 (2)	C(39)	10228 (2)	2991 (2)	4911 (3)	71 (2)
C(5)	8148 (2)	277 (2)	2945 (3)	59 (2)	C(40)	9018 (2)	2297 (2)	5014 (3)	67 (2)
C(6)	7717 (2)	926 (2)	2484 (2)	47 (1)	C(41)	9300 (2)	3280 (1)	-506 (2)	39 (1)
C(7)	6794 (2)	1281 (2)	2671 (3)	65 (2)	C(42)	10265 (2)	3149 (2)	-128 (2)	43 (1)
C(8)	9445 (3)	-768 (2)	3402 (3)	92 (2)	C(43)	10745 (2)	3518 (2)	-557 (3)	60 (2)
C(9)	9492 (2)	1071 (2)	1038 (3)	63 (2)	C(44)	10312 (2)	4008 (2)	-1288 (3)	72 (2)
C(10)	7164 (2)	1066 (1)	-1520 (2)	41 (1)	C(45)	9373 (2)	4136 (2)	-1628 (3)	62 (2)
C(11)	7683 (2)	953 (2)	-2349 (2)	48 (1)	C(46)	8837 (2)	3775 (2)	-1254 (2)	44 (1)
C(12)	7952 (2)	177 (2)	-2989 (3)	65 (2)	C(47)	7809 (2)	3959 (2)	-1678 (2)	49 (1)
C(13)	7742 (2)	-497 (2)	-2852 (3)	72 (2)	C(48)	7406 (2)	3643 (2)	-3084 (3)	73 (2)
C(14)	7211 (2)	-389 (2)	-2085 (3)	67 (2)	C(49)	7530 (2)	4861 (2)	-1228 (3)	72 (2)
C(15)	6917 (2)	373 (2)	-1426 (2)	48 (1)	C(50)	10767 (2)	2614 (2)	683 (2)	50 (1)
C(16)	6307 (2)	408 (2)	-666 (3)	63 (2)	C(51)	11006 (3)	1774 (2)	-59 (3)	89 (2)
C(17)	8076 (3)	-1333 (2)	-3539 (3)	112 (2)	C(52)	11621 (2)	2968 (2)	1675 (3)	83 (2)
C(18)	7926 (2)	1635 (2)	-2637 (3)	67 (2)	C(53)	4948 (2)	1891 (1)	-1941 (2)	41 (1)
C(19)	7683 (2)	4068 (1)	1186 (2)	33 (1)	C(54)	4798 (2)	1618 (2)	-3216 (3)	48 (1)
C(20)	8413 (2)	4479 (1)	2135 (2)	35 (1)	C(55)	4047 (2)	1175 (2)	-3925 (3)	67 (2)
C(21)	8267 (2)	5293 (2)	2741 (2)	42 (1)	C(56)	3468 (2)	1026 (2)	-3397 (3)	80 (2)
C(22)	7429 (2)	5728 (2)	2442 (3)	47 (1)	C(57)	3619 (2)	1324 (2)	-2144 (3)	70 (2)
C(23)	6828 (2)	4515 (1)	872 (2)	37 (1)	C(58)	4359 (2)	1770 (2)	-1371 (3)	48 (1)
C(24)	6722 (2)	5333 (2)	1502 (3)	46 (1)	C(59)	4468 (2)	2158 (2)	-5 (3)	55 (1)
C(25)	6014 (2)	4159 (2)	-148 (3)	52 (1)	C(60)	3911 (2)	2970 (2)	202 (3)	85 (2)
C(26)	7297 (2)	6614 (2)	3136 (3)	80 (2)	C(61)	4231 (2)	1628 (2)	606 (3)	82 (2)
C(27)	9365 (2)	4082 (2)	2512 (2)	43 (1)	C(62)	5382 (2)	1830 (2)	-3836 (3)	62 (1)
C(28)	7639 (2)	3522 (1)	3641 (2)	37 (1)	C(63)	4970 (3)	2571 (3)	-4214 (5)	127 (3)
C(29)	8549 (2)	3569 (1)	4407 (2)	37 (1)	C(64)	5605 (3)	1146 (3)	-4869 (4)	135 (3)

^a Equivalent isotropic U defined as one-third of the trace of the orthogonalized U_{ij} tensor.

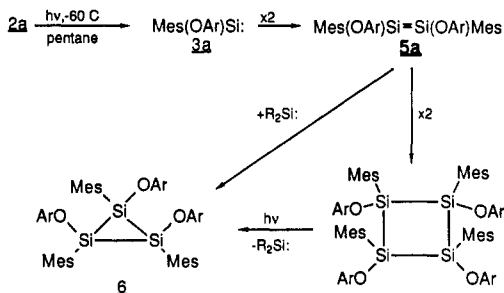


Figure 8. Two possible pathways to formation of 6 from 2a.

could react with a third silylene to form 6 directly or 4a could dimerize to give a four-membered ring. Some perisilacyclobutanes are known to be photolabile, giving cyclotrissilanes and silylenes.¹⁹

Attempts to determine the pathway by which 6 is formed failed to provide evidence for either mechanism. Irradiation of a sample of 2a in a 10-mm quartz NMR tube in pentane at -60°C resulted in the formation of a bright yellow solution. The sample was analyzed by ^{29}Si NMR spectroscopy at -60°C , and no new products other than 6 were observed. Thus, no evidence for a four-membered ring or an intermediate disilene was obtained.

Although the addition of silylene to an olefin is a well-studied reaction, addition of silylene to a silicon-silicon double bond has yet to be documented. Photolysis of 2a in the presence of tetramesityldisilene (7) at -60°C in pentane gave no product of the reaction of silylene 3a with 7; instead, cyclotrissilane 6 was again obtained in nearly quantitative yield.

Experimental Section

General Procedures. All manipulations were carried out under dry nitrogen. The 3-methylpentane (Aldrich) used for matrix studies was deolefinated,²⁰ dried over MgSO_4 , and distilled from LiAlH_4 prior to use. Toluene (NaK), hexane (Na/benzophenone), and THF (Na/benzophenone) used in syntheses were all distilled prior to use. All ^1H NMR spectra were recorded on a Bruker WP-270 NMR spectrometer. ^1H chemical shifts were referenced to the residual protons of C_6D_6 . ^{29}Si and ^{13}C NMR spectra were obtained on a Bruker AM-360 spectrometer. ^{29}Si chemical shifts were referenced to external tetramethylsilane, and ^{13}C shifts were referenced to the C_6D_6 peaks. GC analysis was carried out on a Hewlett-Packard 5890A instrument equipped with a 0.53 mm \times 15 m open tubular column coated with 5% phenylmethylsilicone. Preparative GC work was done on a GOW-MAC Model 550P instrument equipped with a $1/4$ in \times 6 ft column packed with 10% SE-30 on Chromosorb W/AW/DMCS. High-resolution mass spectra were recorded on a Kratos Ms-80 instrument. IR spectra were taken on a Mattson Instrument Polaris FT-IR spectrometer. UV spectra were recorded on a Perkin-Elmer Lambda Array Model 3840 spectrophotometer interfaced with a Motorola Series 7000 computer. Elemental analyses were performed by Galbraith Laboratories, Inc., Knoxville, TN.

All reactions were carried out under an atmosphere of dry nitrogen unless otherwise noted. Glassware was oven-dried overnight. The phenols and alcohols used (Aldrich) were distilled from Na prior to use. Dodecamethylcyclohexasilane was prepared by a literature method.²⁰

2-Mesityl-2-chloro-1,1,3,3,3-hexamethyltrisilane (1). To a flask containing 22.0 g (0.11 mol) of bromomesitylene and 125 mL of diethyl ether was added 180 mL of 1.6 M *n*-butyllithium (0.28 mol) in hexane over 20 min. The solution turned fluorescent green, and a white precipitate formed. The conversion to mesityllithium was measured by the ratio of bromomesitylene to

(19) Watanabe, H.; Kougo, Y.; Nagai, Y. *J. Chem. Soc., Chem. Commun.* 1984, 66.

(20) Chen, S. M.; Katti, A.; Blinka, T. A.; West, R. *Synthesis* 1985, 617, 684.

mesitylene in aliquots of the reaction mixture quenched with water. When the conversion was >80%, the precipitated mesityllithium was filtered and washed with diethyl ether. Mesityllithium was slurried in 200 mL of benzene and added slowly to a refluxing solution of 26.6 g (0.11 mol) of 2,2-dichloro-1,1,1,3,3,3-hexamethyltrisilane in 250 mL of benzene over 1 h, then this mixture was stirred and refluxed. Analysis by GLC showed conversion to product to be complete after 22 h. The benzene was stripped and the residue was fractionally distilled (bp 90 °C (0.1 Torr)) to give 18.8 g (53%) of colorless product. ^1H NMR (benzene): δ 0.15 (s, 18 H), 2.06 (s, 3 H), 2.47 (s, 6 H), 6.66 (s, 2 H). Anal. Calcd for $\text{C}_{15}\text{H}_{29}\text{SiCl}$: Cl, 14.94. Found: Cl, 14.7, 14.6.

A three-necked flask equipped with gas inlet, addition funnel, reflux condenser, and magnetic stirrer was charged with a solution of 5.0 g (15 mmol) of $\text{Mes}(\text{Cl})\text{Si}(\text{SiMe}_3)_2$ in 50 mL of dry THF. The lithium phenoxides were prepared by the method of Shobatake,²¹ filtered, washed with hexane, and dried; then 15 mmol of phenoxide was dissolved in 50 mL of THF and placed in the addition funnel. The phenoxide solution was added slowly to the chlorosilane solution, with stirring, at 25 °C. The mixture was then heated to reflux for 12–15 h. Next, the solution was cooled to room temperature, the THF was removed in vacuo, and the residue was redissolved in hexane. The insoluble LiCl was removed by filtration, and the salts were washed with hexane. The organic fractions were combined and were washed with water, dried over MgSO_4 , and concentrated in vacuo to yield an oil from which crystals formed upon staining at room temperature. Recrystallization from hexane provided the pure trisilanes as colorless air-stable solids.

2-Mesityl-2-(2,6-diisopropylphenoxy)-1,1,1,3,3,3-hexamethyltrisilane (2a). ^1H NMR (C_6D_6): δ 7.05 (d, 2 H), 7.03 (t, 1 H), 6.75 (s, 2 H), 3.25 (sep, 2 H), 2.51 (s, 6 H), 2.10 (s, 3 H), 1.12 (d, 12 H), 0.23 (s, 18 H). ^{29}Si NMR (C_6D_6): δ +4.91, -16.02. MS: $M - 73$ calcd, m/e 397.2373; found, 397.2380. Mp: 132–136 °C. Anal. Calcd for $\text{C}_{27}\text{H}_{46}\text{Si}_3\text{O}$: C, 68.79; H, 9.97. Found: C, 68.43; H, 10.06. Yield: 4.9 g (70%).

2-Mesityl-2-(2,4,6-trimethylphenoxy)-1,1,1,3,3,3-hexamethyltrisilane (2b). ^1H NMR (C_6H_6): δ 6.76 (s, 2 H), 6.67 (s, 2 H), 2.47 (s, 6 H), 2.19 (s, 6 H), 2.11 (s, 3 H), 2.09 (s, 3 H). ^{29}Si NMR (C_6D_6): δ +5.66, -16.21. MS: M calcd, m/e 428.2376; found, m/e 428.2387 (0.57%). Anal. Calcd for $\text{C}_{20}\text{H}_{40}\text{Si}_3\text{O}$: C, 67.29; H, 9.35. Found: C, 66.96; H, 9.42. Mp: 118–122 °C. Yield: 4.2 g.

2-Mesityl-2-phenoxy-1,1,1,3,3,3-hexamethyltrisilane (2c). ^1H NMR (C_6D_6): δ 6.9 (m, 5 H), 6.75 (s, 2 H), 2.40 (s, 6 H), 2.09 (s, 3 H). ^{29}Si NMR (C_6D_6): δ +4.51, -14.82. MS: M calcd, m/e 386.1917; found m/e 386.1903 (0.27%). Anal. Calcd for $\text{C}_{21}\text{H}_{34}\text{Si}_3\text{O}$: C, 65.28; H, 8.81. Found: C, 65.19; H, 8.94. Yield: 4.3 g (75%).

Synthesis of Alkoxytrisilanes 2d, 2e, and 2f. A solution of 1.0 g (3.0 mmol) of $\text{Mes}(\text{Cl})\text{Si}(\text{SiMe}_3)_2$ in 30 mL of hexane was placed into a three-necked flask equipped with a reflux condenser, N_2 inlet, rubber septum, and magnetic stirrer. To this solution was added 4 equiv of Et_3N via syringe, followed by 1.1 equiv of the appropriate alcohol. A voluminous white precipitate was formed upon addition of the alcohol. The mixture was stirred overnight at room temperature. In the case of *t*-BuOH, the mixture was brought to hexane reflux for 14 h. GC analysis at this time showed greater than 90% conversion to the desired alkoxytrisilane. The mixture was filtered, and the salts were washed at least three times with hexane. The organic fractions were combined, washed with water, and dried over Na_2SO_4 , and the solvent was removed in vacuo to yield a viscous oil. The trisilanes were purified by vacuum distillation to yield colorless air-stable oils. NMR spectra (^1H , ^{29}Si) were consistent with the assigned structures and indicated purity to be >95%. Samples for photolysis were further purified by preparative GC.

2-Mesityl-2-methoxy-1,1,1,3,3,3-hexamethyltrisilane (2d). ^1H NMR (C_6D_6): δ 6.75 (s, 2 H), 3.32 (s, 3 H), 2.43 (s, 6 H), 2.12 (s, 3 H), 0.25 (s, 18 H). ^{29}Si NMR (C_6D_6): δ +8.08, -16.65. MS: calcd, m/e 324.1761; found, m/e 324.1757 (4.87%). Bp: 130 °C at 0.5 Torr. Yield: 0.80 g (82%).

2-Mesityl-2-ethoxy-1,1,1,3,3,3-hexamethyltrisilane (2e). ^1H NMR (CDCl_3): δ 6.79 (s, 2 H), 3.61 (q, 2 H), 2.36 (s, 6 H), 2.26 (s, 3 H), 1.20 (t, 3 H), 0.19 (s, 18 H). ^{29}Si NMR (CDCl_3): δ +4.57, -16.81. MS: $M^+ - \text{CH}_3$ calcd, m/e 323.1683; found, m/e 323.1682 (no parent peak was observed). Bp: 135 °C at 0.5 Torr. Yield: 0.70 g (70%).

2-Mesityl-2-tert-butoxy-1,1,1,3,3,3-hexamethyltrisilane (2f). ^1H NMR (CDCl_3): δ 6.72 (s, 2 H), 2.46 (s, 6 H), 2.21 (s, 3 H), 1.15 (s, 9 H), 0.18 (s, 18 H). MS: $M - 57$ calcd, m/e 309.1526; found, m/e 309.1521 (no parent peak was observed). Bp: 142 °C at 0.5 Torr. Yield: 0.50 g (45%).

Photolysis of Trisilanes 2a–2f at 77 K in 3-MP. In a typical experiment, 1 mg of trisilane was dissolved in 1 mL of 3-MP in a Suprasil cuvette; the sample was degassed by three freeze-pump-thaw cycles. The cuvette was then placed in a quartz-windowed dewar filled with liquid nitrogen. The glass formed was then irradiated for 15–30 min in a Rayonet RPR-208 photoreactor equipped with low-pressure mercury lamps. After the UV spectrum was recorded, the liquid nitrogen was removed and the UV spectrum was monitored as the matrix annealed. For silylenes **3a** and **3b**, the glass was quickly recooled to 77 K after the shift in the UV maximum was observed. This had no effect on the new absorption. Irradiation of the matrix with visible light following the anneal-recool sequence also had no effect on the position of the absorption band.

Trapping Experiments in 3-MP. In a typical experiment, 1 mg of trisilane was dissolved in 1 mL of solvent (3-MP, 1:1 3-MP/isopentane, 4:1 3-MP/isopentane). To this was added a 20-fold excess of EtOH. The sample was prepared as described above and irradiated at 254 nm for 15–30 min. The UV spectra taken following photolysis were identical with those obtained in pure 3-MP. The sample was then taken through 10–15 freeze-irradiate-thaw cycles. Next, the solution was analyzed on a Kratos MS-25 GC/MS instrument to detect the presence of the insertion products **4a–4f**.

Solution Photolysis of 2a. To a quartz photolysis vessel was added 60 mg of **2a** (1.28×10^{-4} mol) and 5 mL of photograde pentane. The solution was degassed, placed into a quartz dewar vessel, cooled to -66 °C, and photolyzed at 254 nm for 8 h. The now bright yellow solution was evaporated in vacuo to yield a darker yellow, air-stable residue. Analysis of the residue by TLC with hexane as the eluant showed that one new product was formed. The residue was chromatographed with Si-60 as the stationary phase and hexane as the mobile phase. Two bands were collected, the first of which contained unreacted starting material. The yellow second fraction was concentrated and cooled to -20 °C. Yellow, rectangular crystals formed overnight and were collected by filtration and recrystallized from hexane to yield 10 mg (25%) of **6**. ^1H NMR (C_6D_6): δ 7.05–6.83 (m, 9 H), 6.56 (s, 1 H), 6.50 (s, 2 H), 6.29 (s, 1 H), 3.65–3.39 (m, 6 H), 2.77 (s, 12 H), 2.23 (s, 6 H), 1.96 (s, 3 H), 1.94 (s, 6 H), 1.21 (d, 12 H), 1.09 (d, 12 H), 0.92 (br, 12 H). ^{29}Si NMR (C_6D_6): δ +7.34, +7.32. Mp: 213–215 °C. Anal. Calcd for $\text{C}_{63}\text{H}_{84}\text{Si}_3\text{O}_3$: C, 77.72; H, 8.70. Found: C, 77.46; H, 8.79.

Photolysis of 6 in C_6D_{12} at Room Temperature. A sample of 10 mg of **6** was dissolved in 0.75 mL of C_6D_{12} and the solution placed in a quartz NMR tube. The sample was degassed, sealed, and irradiated for 1 h. ^{29}Si NMR and ^1H NMR spectra were then acquired (AM-360). No products were isolated from this reaction.

Low-Temperature NMR Analysis of the Photolysis of 2. A sample of 100 mg (2.1×10^{-4} mol) of **2** was dissolved in 2 mL of pentane. The solution was placed into a 10-mm quartz NMR tube and degassed and the tube sealed. The mixture was then irradiated with 254-nm light at -60 °C for 12 h. At this time the solution was bright yellow. The NMR tube was transferred quickly to the precooled probe of the NMR spectrometer. ^{29}Si NMR analysis with use of the INEPTD pulse sequence was then attempted at -60 °C. The spectrometer was tuned before the sample was introduced and was then run unlocked.

X-ray Crystallography of 2a, 2c, and 6. Crystals of each compound suitable for X-ray analysis were obtained from hexane. Data collection for **2c** was done on a Nicolet P1 diffractometer equipped with a modified LT-1 low-temperature device. For **2a** and **6** data collection was done on a Nicolet P3/F diffractometer. Unit cell parameters were determined by least-squares refinements based on 25 centered reflections. Four standard reflections

representing diverse regions of reciprocal space were monitored every 100 reflections during data collection. Little deviation in peak intensities was observed during data collection, and no absorption corrections were applied.

The structures were solved by direct methods with the SHELXTL software package. In all three structures, most of the atoms were located in the *E* maps; the remaining atoms were found in subsequent difference electron density maps. Blocked-cascade least-squares refinements of the structures used the reflections with $F_o > 3\sigma(F_o)$. Atomic form factors were taken from standard sources.²² In the final refinement cycles the non-hydrogen atoms

were assumed to vibrate anisotropically while the hydrogen atoms were included as idealized isotropic fixed contributors (C-H bond length 0.96 Å, $U(\text{hydrogen}) = 1.2[U(\text{carbon})]$). The final discrepancy indices R_1 and R_2 are given in Table II.

Acknowledgment. This work was supported by the Air Force Office of Scientific Research Air Force Systems Command, USAF, under Contract No. F49620-86-0010 and by the National Science Foundation Grant No. CHE-8318810-02.

Supplementary Material Available: Tables of hydrogen atom coordinates and anisotropic thermal parameters for **2a**, **2c**, and **6** (8 pages); listings of observed and calculated structure factor amplitudes for **2a**, **2c**, and **6** (72 pages). Ordering information is given on any current masthead page.

(22) Atomic form factors from: Cromer, D.; Waber, J. *International Tables for X-ray Crystallography*; Kynoch Press: Birmingham, England, 1974; Vol. 4, pp 99-101, Table 2.2B. Atomic form factor for hydrogen from: Stewart, R.; Davidson, E.; Simpson, W. *J. Chem. Phys.* 1985, 42, 3175. Anomalous scattering components from: Cromer, D.; Liberman, D. *J. Chem. Phys.* 1970, 53, 1981.

Further Illustration of the Versatility of the Alkynylphosphines $\text{Ph}_2\text{P}(\text{C}\equiv\text{CR})$ toward $[\text{PPh}_4][\text{HFe}_3(\text{CO})_{11}]$ When $\text{R} = \text{H}$, $\text{C}(\text{O})\text{OMe}$

Dolors Montlo and Joan Suades

Departament de Química, Divisió Inorgànica, Universitat Autònoma de Barcelona, Bellaterra, 08193 Barcelona, Spain

Françoise Dahan and René Mathieu*

Laboratoire de Chimie de Coordination du CNRS, UPR 8241 liée par conventions à l'Université Paul Sabatier et à l'Institut National Polytechnique, 205 route de Narbonne, 31077 Toulouse Cedex, France

Received January 31, 1990

The alkynylphosphines $\text{Ph}_2\text{P}(\text{C}\equiv\text{CR})$ ($\text{R} = \text{H}$, $\text{C}(\text{O})\text{OMe}$) react with $[\text{PPh}_4][\text{HFe}_3(\text{CO})_{11}]$ to give, in a first step, complexes containing the $\text{Ph}_2\text{PC}=\text{CHR}$ ligands. When $\text{R} = \text{C}(\text{O})\text{OMe}$, the structure of the complex **3** isolated was determined by a single-crystal X-ray diffraction study. The anionic part consists of a $\text{Ph}_2\text{PC}=\text{CHC}(\text{O})\text{OMe}$ ligand in which the phosphorus atom is bonded to an $\text{Fe}(\text{CO})_4$ group and in which the $\text{C}=\text{CHC}(\text{O})\text{OMe}$ fragment is η^1, η^2 -bonded and $\eta^1(\text{O})$ -bonded to an anionic $\text{Fe}_2(\text{CO})_6$ unit. When $\text{R} = \text{H}$, the structure of complex **5** was deduced from spectroscopic data. It consists of a Ph_2PCCH_2 ligand bonded to each iron atom of an $[\text{Fe}_3(\text{CO})_9]^-$ triangle through the P, C, and $\text{C}=\text{CH}_2$ atoms, respectively. Complexes **3** and **5** evolved in boiling acetone and ethyl acetate, respectively, to $[\text{PPh}_4][\text{Fe}_3(\text{CO})_6(\mu\text{-CO})_2(\mu\text{-PPh}_2)(\mu\text{-CCHR})]$ compounds, resulting from the breaking of the phosphorous-carbon bond.

Introduction

Previous studies by Carty¹ and Sappa² have shown the great reactivity of alkynylphosphines toward polynuclear complexes. The reactions observed generally imply the breaking of the phosphorus-alkynyl bond and, in some cases, the reaction of the acetylide fragment generated with either hydride³ or hydrocarbon ligands bonded on the polymetallic frames.² The backformation of a PPh_2 -carbon bond has even been observed.^{2,4}

We have recently shown that the reactivity of alkynylphosphines $\text{Ph}_2\text{PC}\equiv\text{CR}$ with $[\text{PPh}_4][\text{HFe}_3(\text{CO})_{11}]$ (**1**) is

also very versatile and dependent on the R group. For instance, when $\text{R} = \text{Me}$, Ph , we have observed the transformation of the phosphine into the $\text{PhPC}(\text{R})\text{CH}(\text{Ph})\mu^3\text{-}\eta^1, \eta^2$ -bonded phosphido ligand.⁵ When $\text{R} = t\text{-Bu}$, one product of the reaction, $[\text{PPh}_4][\text{Fe}_3(\text{CO})_6(\mu\text{-PPh}_2)(\mu\text{-CO})_2(\mu\text{-CCH}(t\text{-Bu}))]$ (**A**), results from the breaking of the phosphorus-alkynyl bond and transformation of the acetylide into a $\mu^3\text{-}\eta^2$ -bonded vinylidene ligand. As for the other product of the reaction, there is formation of the $\text{Ph}_2\text{PCH}=\text{C}(\text{CMe}_3)\text{C}(\text{O})$ ligand⁶ bonded to a $\text{Fe}_2(\text{CO})_6$ unit. This dependence of the reactivity on the R group has led us to increase the field of this study to the case when $\text{R} = \text{H}$ and $\text{R} =$ electron-withdrawing group.

For this reason we have synthesized the phosphine $\text{Ph}_2\text{PC}\equiv\text{CC}(\text{O})\text{OMe}$, which, to our knowledge, has never been described before. Reaction with $[\text{PPh}_4][\text{HFe}_3(\text{CO})_{11}]$

(1) Nucciarone, D.; McLaughlin, S. A.; Taylor, N. J.; Carty, A. *J. Organometallics* 1988, 7, 106 and references therein.

(2) Sappa, E.; Pasquinelli, G.; Tiripicchio, A.; Tiripicchio Camellini, M. *J. Chem. Soc., Dalton Trans.* 1989, 601 and references therein.

(3) Van Gestel, F.; McLaughlin, S. A.; Lynch, M.; Carty, A. J.; Sappa, E.; Tiripicchio, A.; Tiripicchio Camellini, M. *J. Organomet. Chem.* 1987, 326, C65.

(4) Fogg, D. E.; McLaughlin, S. A.; Kwek, K.; Cherkas, A. A.; Taylor, N. J.; Carty, A. *J. Organomet. Chem.* 1988, 352, C17.

(5) Montlo, D.; Suades, J.; Torres, M. R.; Perales, A.; Mathieu, R. *J. Chem. Soc., Chem. Commun.* 1989, 97.

(6) Suades, J.; Dahan, F.; Mathieu, R. *Organometallics* 1989, 8, 842.